Transactions of the Korean Nuclear Society Spring Meeting
Jeju, Korea, May 22-23, 2025

MTC Effect with Axial Cutback for Controlling Secondary Reactivity Based on Coolant Temperature during the Load-Follow Operation

Yu Yeon Cho [a], Chang Hee Lee [a], Han Seung Song [a], Junggyu Lee [a]
[a]*KEPCO Nuclear Fuel, 242, Daedeok-daero 989 beon-gil, Yuseong-gu, Daejeon 34057, Republic of Korea*
[*]*Corresponding author: yycho@knfc.co.kr*

Keywords : i-SMR, Secondary reactivity control, Moderator Temperature Coefficient, Axial cutback

1. Introduction

The Innovative-Small Modular Reactor (i-SMR) will introduce the primary coolant temperature control as a secondary reactivity control method. In a soluble boron-free core, a significantly large negative moderator temperature coefficient (MTC) can lead to large reactivity feedback [1].

At our previous study, the effect of MTC on the reactivity control was analyzed by changing the axial cutback length for BOC of the initial core cycle (1st cycle) only. As the axial cutback size increases, MTC becomes more negative, leading to a reduction in the temperature range during load-follow operation [2].

In this work, we designed different lengths of the axial cutback to analyze the effect of MTC on secondary reactivity control during the load-follow operation for BOC, MOC and near EOC of the equilibrium core cycle (8th cycle). The reactivity variation due to power change and required coolant temperature change on the RCS temperature control were evaluated.

2. Methods and Results

2.1 Computational Methods

Assembly burnup calculations for two group cross section generation were calculated by KARMA (Kernel Analyzer by Ray-tracing Method for fuel Assembly) [3, 4] which is a two-dimensional multi-group lattice transport code. KARMA includes the ENDF/B-VI.8 based 190 group and 47 group cross section library. This code uses the subgroup method for resonance self-shielding effect and MOC (Method of Characteristics) as the transport solution method.

ASTRA (Advanced Static and Transient Reactor Analyzer) code was used for three-dimensional core calculation [5]. This code is a 3D core depletion code and developed by KEPCO NF (KEPCO Nuclear Fuel) as a nuclear design code for the core design of pressurized water reactors (PWRs) based on the reactor physics technologies. It adopts a Semi-Analytic Nodal Method (SANM) formulated with the Coarse-Mesh Finite Difference method (CMFD) as the neutronics solver for the reactor core analysis [6, 7].

2.2 Core design and performance analysis

The i-SMR is designed for a thermal power output of 520 MW. The core consists of 69 assemblies arranged in a 17 × 17 lattice. The active core height is 240 cm divided into 24 axial meshes. In the reference model (Case 2), each assembly features a 20 cm top cutback region to control axial power distribution, with 2.2 wt.% uranium enrichment. For a sensitivity analysis of the MTC effect, additional cases of 10 cm (Case 1), 30 cm (Case 3), and 40 cm (Case 4) were considered. The core layouts are the same as the previous work [2].

Table I shows Isothermal Temperature Coefficient (ITC) versus burnup change for 8th cycle. Since ITC accounts for both fuel and coolant temperature changes, it was used to calculate the coolant inlet temperature necessary for load-follow operation without control rod movement, offering a more accurate assessment compared to MTC, which only considers the coolant changes.

ITC was calculated at HFP for BOC, MOC, and near EOC (18,000 MWD/MTU). As the cycle length varies depending on the axial cutback length, calculations were performed at near EOC to allow for comparisons at a same burnup point.

In all cases, ITC became less negative until the MOC and then turned more negative. As burnup progressed, multiple factors including the accumulation of fission products, and change in the axial power distribution influenced ITC. Consequently, ITC did not change in a consistent direction with burnup.

At BOC, the maximum difference in ITC among cases was up to ~3 pcm/°C. As the axial cutback increased, the gadolinium contents decreased, leading to a more negative ITC. However, at MOC and near EOC, the difference was significantly reduced to a maximum of 0.217 pcm/°C. The depletion of gadolinium resulted in a decrease in neutron absorption by the burnable poison, leading to reducing its effect on ITC.

Overall, ITC tends to be more negative as the axial cutback increases. However, at near EOC, the trend reverses for the Case 3 and the Case 4, with values of -65.723 pcm/°C and -65.717 pcm /°C, respectively.

Table I. ITC versus burnup change

	Case 1	*Case 2*	*Case 3*	*Case 4*
Cutback [cm]	10	20	30	40
BOC [pcm/°C]	-61.740	-62.011	-62.859	-64.734
MOC [pcm/°C]	-59.647	-59.679	-59.771	-59.806
Near EOC [pcm/°C]	-65.506	-65.623	-65.723	-65.717

MTC versus burnup change for 8th cycle is summarized in Table II. Due to nearly constant value of the Fuel Temperature Coefficient (FTC) across all cases, the behavior of MTC and ITC followed nearly the same trend. However, unlike ITC, MTC shows a consistent trend of becoming slightly negative with increasing the length of the axial cutback throughout the entire cycle.

Table II. MTC versus burnup change

	Case 1	*Case 2*	*Case 3*	*Case 4*
Cutback [cm]	10	20	30	40
BOC [pcm/°C]	-58.705	-58.964	-59.790	-61.649
MOC [pcm/°C]	-56.477	-56.500	-56.583	-56.610
Near EOC [pcm/°C]	-62.249	-62.365	-62.469	-62.474

2.3 Analysis of reactivity variation due to power change

A change in core power results in the corresponding changes in thermal and fast neutron flux distribution, which causes the reactivity variations due to xenon concentration changes and the power defect, which results from the combined feedback of moderator and fuel temperature changes [8].

We considered the following power control strategy of the daily load follow operation: The core power decreased from 100% to 50% over 2 hours, held at 50% for 4 hours then returned to 100% over 2 hours and held for 16 hours. Under the condition of control rods being fixed at the initial critical state, this evaluation involved calculating eigenvalues corresponding to power changes over time.

Fig. 1, 2 and 3 show that the net change of reactivity with the power change at BOC, MOC and near EOC, respectively. The excess reactivity change patterns at BOC and MOC are similar, whereas at near EOC, the reactivity exhibits a larger variation with power changes.

As shown in Fig. 1, the maximum net change of reactivity at BOC reached 335 pcm in the Case 1, while 300 pcm was observed in the Case 4, which is the lowest value among the cases. At MOC with Fig. 2, the Case 1 and the Case 4 showed the maximum net change of reactivity of 330 pcm and 311 pcm, respectively, which are the highest and lowest excess reactivity.

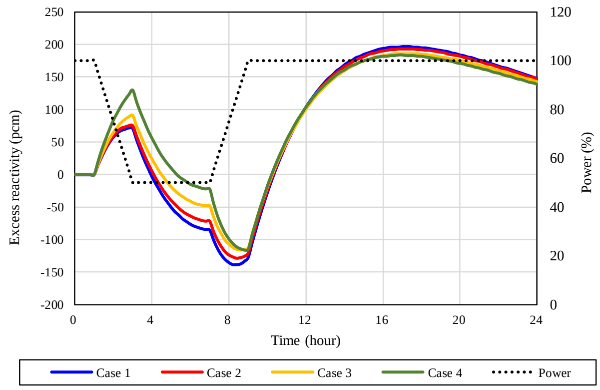

Fig. 1. The reactivity variation with power change (BOC)

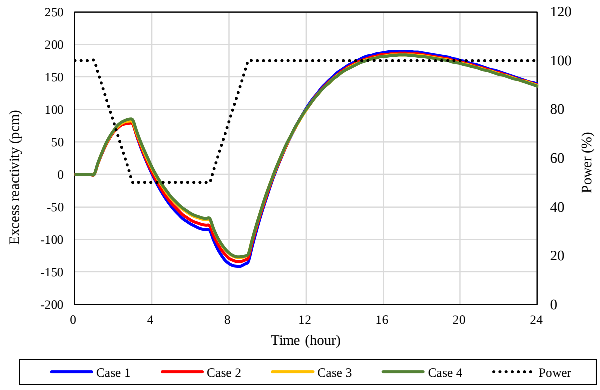

Fig. 2. The reactivity variation with power change (MOC)

Fig. 3 shows that the net change of reactivity with the power change at near EOC. Unlike the pattern observed at Fig. 1 and 2, the largest variation was observed in the Case 4, with a reactivity net change of 364 pcm. It is estimated to be in a range of +198 pcm to -166 pcm. At near EOC, unlike BOC and MOC, an increased axial cutback leads more bottom-skewed axial power distribution, resulting in a higher net reactivity.

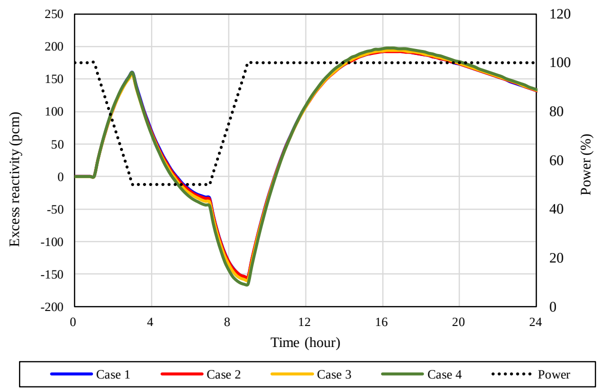

Fig. 3. The reactivity variation with power change (near EOC)

2.4 Daily Load follow Operation using Coolant Temperature Change

As described in Section 2.3, the power control strategy follows a 100-50-100% power pattern with a 2-4-2-16 hour daily load-follow operation.

Fig. 4 illustrates the changes of the inlet temperature during the load-follow operation at BOC. The programmed inlet temperature for each case represents the required inlet temperature to sustain reactivity without control rod movement. The maximum changes with the reference temperature and the controlled temperature, required for daily load follow operation, are ±3.13°C and ±2.67°C for the Case 1 and the Case 4, respectively.

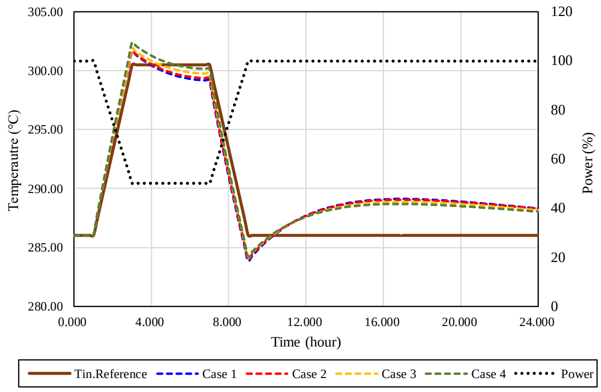

Fig. 4. Temperature change during load follow (BOC)

Table III shows the performance parameters at BOC. As the axial cutback increases, the axial power distribution tends to become more top-skewed, leading to a decrease in the net reactivity change and consequently reducing the temperature variation.

Table III. Summary of performance parameters (BOC)

	Case 1	***Case 2***	***Case 3***	***Case 4***
Maximum excess reactivity [pcm]	197	193	186	184
Minimum excess reactivity [pcm]	-138	-129	-116	-116
Net change of reactivity [pcm]	335	322	302	300
Temperature change [°C]	±3.13	±3.03	±2.85	±2.67

Fig. 5 illustrates the changes of the inlet temperature during the load-follow operation at MOC. The maximum changes with the reference temperature and the controlled temperature, required for daily load follow operation, are ±3.09°C and ±2.95°C for the Case 1 and the Case 4, respectively.

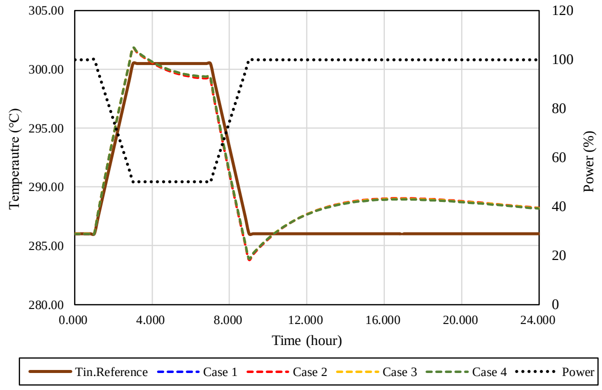

Fig. 5. Temperature change during load follow (MOC)

Table IV shows the performance parameters at MOC. Similar to the trend observed at BOC, an increase of the axial cutback leads to more top-skewed axial power distribution. Both the net change of reactivity and the temperature variation show a decrease.

Table IV. Summary of performance parameters (MOC)

	Case 1	***Case 2***	***Case 3***	***Case 4***
Maximum excess reactivity [pcm]	189	187	184	184
Minimum excess reactivity [pcm]	-141	-134	-128	-127
Net change of reactivity [pcm]	330	321	312	311
Temperature change [°C]	±3.09	±3.04	±2.98	±2.95

Fig. 6 depicts the changes of the inlet temperature during the load-follow operation at near EOC. The maximum temperature changes required for daily load follow operation, are ±2.82°C, ±2.80°C, ±2.83°C and ±2.89°C for the Case 1 to the Case 4, respectively. Unlike the trend in the MOC, the effect of the axial cutback length did not follow a constant pattern.

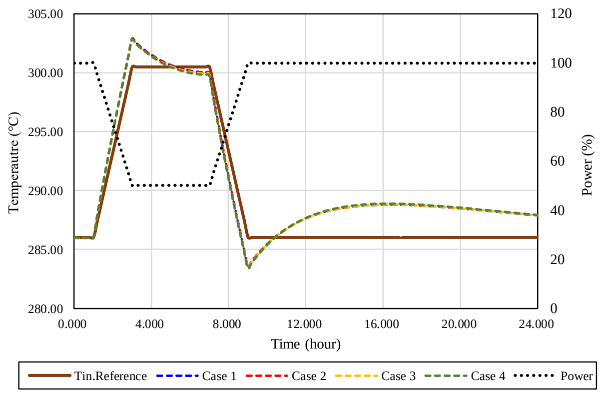

Fig. 6. Temperature change during load follow (near EOC)

The performance parameters at near EOC are summarized in Table V. Although the ITC in the Case 4 was the most negative, it resulted in the largest net change of reactivity and temperature change. As burnup progresses, the difference in MTC among cases becomes minimal, and the temperature control range also showing a very small variation of ±2.80–2.89°C.

Table V. Summary of performance parameters (near EOC)

	Case 1	***Case 2***	***Case 3***	***Case 4***
Maximum excess reactivity [pcm]	193	192	194	198
Minimum excess reactivity [pcm]	-155	-155	-159	-166
Net change of reactivity [pcm]	348	347	353	364
Temperature change [°C]	±2.82	±2.80	±2.83	±2.89

Table VI summarizes the maximum temperature control range for each case. Each calculated value represents the highest temperature change among the load-follow operations at BOC, MOC, and EOC. The Case 1 exhibited the largest temperature control range at ±3.13°C, while the Case 4 showed the smallest at ±2.95°C.

Table VI. Maximum temperature control range

	Case 1	***Case 2***	***Case 3***	***Case 4***
Maximum temperature change [°C]	±3.13	±3.04	±2.98	±2.95

3. Conclusions

The effect of MTC in reactivity control was analyzed by changing the axial cutback length for BOC, MOC and near EOC of 8^{th} cycle. Due to gadolinium depletion and the complex power distribution of a soluble boron-free core, ITC exhibits irregular changes over burnup.

A longer axial cutback resulted in a more negative MTC. The net reactivity change and temperature variation were both reduced as the axial cutback increased at BOC and MOC. In contrast, at near EOC, the longest axial cutback of 40 cm required the largest temperature control range.

The study confirmed that variations in axial cutback length and core configuration impacted MTC, resulting in changes in power distribution and modifications in the required temperature control range. Compared to the reference case, which has the axial cutback of 20 cm, it was observed that the temperature control range decreased as the axial cutback increased.

In the future work, the temperature coefficients of the soluble boron-free core will be physically analyzed in detail to further optimize the MTC.

Acknowledgement

This work was supported by the Innovative Small Modular Reactor Development Agency grant funded by the Korea Government (MOTIE) (No. RS-2024-00405419).

REFERENCES

[1] L. van der Merwe and C. J. Hah, "Reactivity balance for a soluble boron-free small modular reactor", Nuclear Engineering and Technology, Vol. 50, p. 723-731, Jul. 2018.
[2] Y. Y. Cho et al., "The Analysis of the MTC Effect for Controlling Secondary Reactivity Based on Coolant Temperature for Soluble Boron-free SMR Core", Transactions of Korea Nuclear Society Autumn Meeting (2024).
[3] K. S. Kim et al., "Transport Lattice Code KARMA 1.1," Transactions of Korea Nuclear Society Autumn Meeting (2009).
[4] K. S. Kim et al., "Implementation of the Gamma Transport Calculation Module in KARMA 1.2", Transactions of Korea Nuclear Society Spring Meeting (2011).
[5] T. Y. Han et al., "Verification of ASTRA Code with PWR MOX/UO2 Transient Benchmark Problem", Transactions of Korea Nuclear Society Autumn Meeting (2010).
[6] J. I. Yoon and H. G. Joo, "Two-Level Coarse Mesh Finite Difference Formulation with Multigroup Source Expansion Nodal Kernels", Journal of Nuclear Science and Technology, Vol. 45, p.668-682 (2008).
[7] H. G. Joo et al., "Multigroup pin power reconstruction with two-dimensional source expansion and corner flux discontinuity", Annals of Nuclear Energy, Vol. 36, p.85~97 (2009).
[8] Junggyu Lee et al., "The Feasibility of Controlling Secondary Reactivity Based on Coolant Temperature for Soluble Boron-free Operation", Transactions of Korea Nuclear Society Spring Meeting (2024).